Characterizing a distributed pressure sensor built from off-the-shelf piezoresistive polymer

TJ Wiegman[a]
Honors Program, Department of Physics & Engineering, Point Loma Nazarene University
(Dated: April 24, 2020)

Measuring the distribution of mechanical pressure across a surface is useful in a wide variety of applications, but traditional measurement tools are either very expensive or single-use. Here we characterize a flexible, reusable sensor built from off-the-shelf materials that is simple and low-cost, but unsuited for high-precision work.

I. PROJECT MOTIVATION

A. Background

One of the most interesting challenges in aerospace engineering is that of the extravehicular activity (EVA) pressure garment, or "space suit". This device must perform all the functions of a complete spacecraft, such that it can sustain a human being in the space environment without needing any connection to another system. Beyond that lofty standard, for maximal usefulness it must also be as svelte and lightweight as possible, to give the operator the greatest freedom of movement such that their productivity is not hindered during their limited EVA time.

The human body requires external pressure in order to properly function; this pressure is provided in the natural environment by the Earth's atmosphere. In current state-of-the-art space suit designs, this pressure is provided by an artificial atmosphere inside the innermost layer of the suit. However, that mechanism is fundamentally limited in its ability to scale down and become less encumbering to the wearer due to the geometry of the human body. As a result, gas-pressurized space suits are "rigid, heavy, bulky, costly, leaky, and require high maintenance"[1].

However, the human body does not require the external pressure to be applied by a gas. An alternative method is to use mechanical counterpressure, the normal force of a solid—such as a tight-fitting garment—instead. While that methodology had been proposed as early as the 1960s[2], research only began in earnest in the last decade, as advances in materials science made the concept significantly more viable[3].

B. Narrowing Scope

Initially, this project aimed to test a simplified model of a novel mechanical counterpressure garment concept. Such a study would have necessitated integrating three major components into one experimental design. First, the garment model itself, which was 3D-printed out of rigid plastic. Second, actuators that could alter the shape of the garment when connected to power, which would make it easier to don or doff the garment by tightening down only when needed—a critical part of modern counterpressure garment design. Thirdly, a pressure sensor array, which could measure the pressure applied by the garment and the distribution of that pressure.

The garment model was not too difficult to construct on a small scale, as the technology chosen for the experiment (3D printing) was exceptionally well suited to rapid prototyping and iteration. In fact, a reasonable specimen was actually produced. Unfortunately, the actuators chosen for the experiment were less easy to work with, requiring exotic materials and specialized tooling to properly form into fully functional components. Due to these factors, the author found that incorporating such a system was too ambitious for a two-semester honors project, and the use of such actuators was reluctantly dropped from the project goals.

Most significant to the project trajectory was the final piece of the experiment, the pressure sensor array. Commercial solutions for this task exist, but, as discussed in more detail in the following section, they prove impractical for a small, low-budget project such as this study. As a result, the author decided to attempt building a custom sensor just for the project. Because this task ended up being a rather significant labor in and of itself, and because the garment model was much less relevant to aerospace applications without the proper actuators, the project was pivoted away from testing the pressure garment design in favor of focusing solely on characterizing the pressure sensor, an extensive experiment in its own right.

In hindsight, it is clear that the original project goals were much too ambitious for a single full-time student to complete in only two semesters. Properly using all three components of the initial experimental design would be the work of something like three or four projects, as each component requires independent testing and verification before it could be integrated into a rigorous experiment with the other components.

---

[a] twiegman2020@pointloma.edu

II. INTRODUCTION

The distribution of pressure across a surface is a useful value to know for a very wide range of applications, from medical technology[4][5][6] to ergonomics[7][8] to robotics[9][10][11][12].

However, the leading traditional sensors for pressure measurements are either very expensive[13] or single-use[14]. While an array of point sensors can be used in place of these, usually based on either strain gauges[15], fiber optics[16], or microelectromechanical systems (MEMS)[12][17], they must either measure at a much coarser resolution or be arranged in a very dense, unwieldy network. Additionally, these devices are usually very rigid and bulky[18], which is a disadvantage when measuring pressure along a curved, irregular, soft, or malleable surface—such as, for example, the interface between a garment and the person wearing it.

This paper presents a flexible, polymer-based distributed piezoresistive pressure sensor that is fabricated exclusively from simple materials that are commercially available in bulk quantities at very low cost. The design is straightforward and robust, and the resulting sensors have several qualities that can make them desirable for applications where existing sensors would be impractical or too expensive for widespread adoption.

III. MATERIALS & METHODS

A. Sensor Fabrication

The sensor was based around a conductive, piezoresistive polymer sheet of plastic that is commercially available under the brand names "Velostat" or "Linqstat"[19]. To measure the resistance at multiple points on the sensor, a lattice of thin copper strips was applied to each side of the film and fixed in place with clear tape. The process of creating the copper electrodes is shown in Figure 1 and the construction of the sensor is shown in Figure 2 and Figure 3.

An Arduino microcontroller was used to control which row of the lattice was being measured and to record the output of each point on the sensor, connected as shown in the circuit in Figure 4. The source code for the microcontroller firmware is published online[20].

B. Verification and Validation

In order to test the sensor's accuracy and precision, each "pixel" (point of overlap between the two layers of the electrode lattice, as shown in Figure 3d) was exposed to a known pressure, given three seconds to settle on a value, and the sensor output was recorded. To apply a known pressure, a three-legged platform was 3D-printed, and one leg was allowed to rest on the sensor while the other two legs rested on a test stand held level with the sensor. The total mass of the platform and any test masses placed on top was recorded. The pressure applied was calculated as the total mass (ranging from 30 to 930 g) divided by the surface area of the platform's feet (3 cm^2). The entire setup is shown in Figure 5.

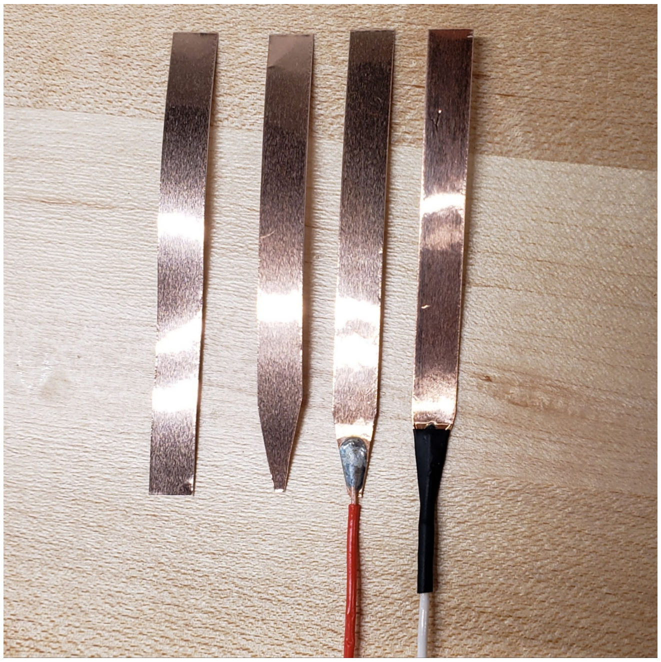

FIG. 1: The lattice of copper strips was created by cutting pieces of thin copper tape into shape, soldering a wire connector to the strip, and then insulating the junction with heatshrink tubing, as shown from left to right in this photograph.

To collect data, each leg of the three-legged platform was placed on the sensor pixel being tested in turn, three times, for a total of nine trials per pressure level per sensor pixel, in order to minimize the effects of any non-uniformity in the legs of the platform.

C. Data Analysis

Data was copied from handwritten records into an electronic spreadsheet, then imported into the R programming language[21]. Analysis was performed according to a script published online[20]. The arithmetic mean and variance were calculated for each pressure level of each sensor, and the standard deviation was used as the uncertainty in the value of the mean. Regression analyses were used to determine pressure's effect on the sensor output, and the method of propagation of error was used to determine the uncertainty in the regression coefficients. The figures generated by this process are attached at the end of this report.

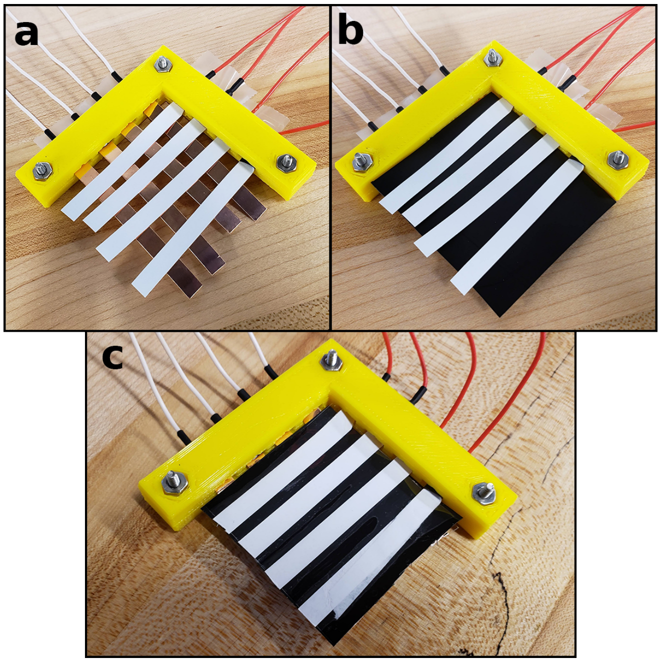

FIG. 2: Photographs of the construction process for the sensor tested in this paper: (a) Eight electrodes were arranged in a lattice shape and held in position with a 3D-printed frame (for strain relief). (b) A sheet of velostat was cut to approximate size and inserted between the two layers of electrodes. (c) The layers were fixed together with clear packing tape and the non-sensing regions on the edges were trimmed away.

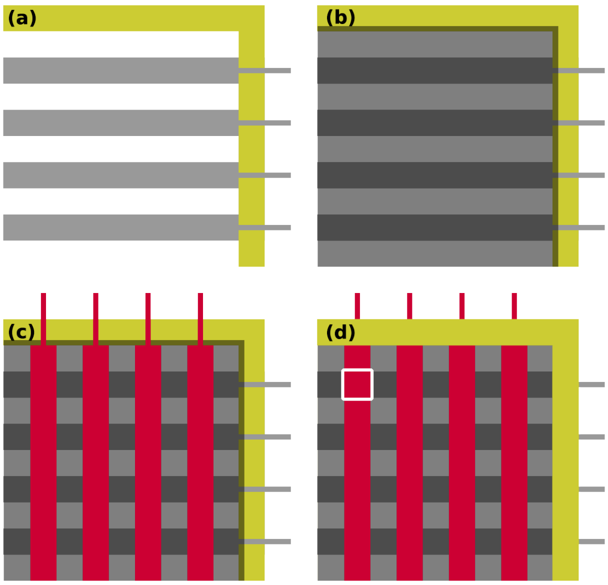

FIG. 3: The layers of the sensor shown as a simplified schematic, from bottom to top: (a) Horizontal electrodes placed into the bottom half of the 3D-printed (strain relief) frame. (b) Velostat sheet on top of those electrodes. (c) Vertical electrodes on top of the velostat sheet. (d) Top half of the strain-relief frame bolted on top. Also in this image, one of the sensor “pixels” is marked with a white box.

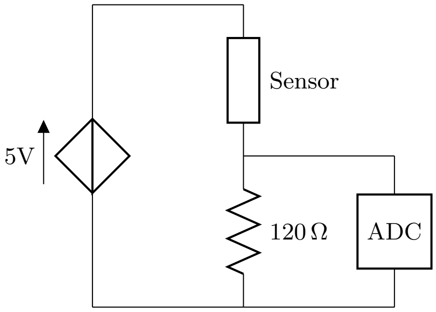

FIG. 4: The general circuit for each sensor pixel. The microcontroller switches on the 5 V supply (left) to activate the pixel, then uses the analog-to-digital converter (ADC) to measure the voltage across the 120 Ω resistor, which increases as the pressure on the sensor increases.

IV. DATA & ANALYSIS

The mean and variance was calculated for each pressure level of each sensor, then plotted for each sensor in Figure 7. Based on the general shape of the response curves, the author suspected a square-root relationship between the sensor output and the pressure input, so a similar plot for the square of the sensor output was made as well (Figure 8).

Examining the plots of the square of the sensors’ output, there appears to be a linear trend at lower pressures, with the values leveling off after about 200 to 250 g/cmˆ2. Based on this observation, a linear trend was fitted to the first seven pressure levels for each center and plotted in Figure 9. The values for the regression coefficients are displayed in Figure 6.

V. RESULTS

For most pixels of the sensor, the square of the output can be predicted with reasonable accuracy for lower pressure values using the regression coefficients for that specific pixel. This is seen in Figure 9, where the regression line fits within the uncertainty of each point with only 32 exceptions among the 112 points: the regression model makes inaccurate predictions about 28% of the time. (N.B.: Many of those 32 missed predictions are clustered in a few pixels, notably five in pixel G and pixel O and four in pixel A; the overall error rate could likely be reduced by using a different model for these pixels).

However, the regression coefficients are significantly different, as seen in Figure 6, varying greatly from pixel to pixel on the sensor. This means that each pixel must be calibrated separately for each sensor built according to this design, otherwise readings from one pixel cannot be compared to those from another, even if they are from the same sensor.

VI. DISCUSSION

A. Interpreting the Results

This sensor design is appealing because it is simple, flexible, and low-cost, since it is made from readily available off-the-shelf materials. However, the accuracy of the sensor varies widely from pixel to pixel, and this lack of accuracy can only be partially remedied by careful calibration. As a result, it is profoundly unsuited for high-precision measurements. Additionally, the need to calibrate each pixel of each sensor individually would make the mass-production of this kind of sensor significantly more challenging than for an architecture where the same calibration could be applied for many sensors made in a batch. For small-quantity use, though, as in hobbyist and cottage-industry products, or for applications where only a rough description of the pressure distribution is needed, this kind of sensor could be an excellent option.

B. Potential Sources of Error

There appear to be two main sources of error and variability in the measurements taken during this experiment (beyond any inherent variability over time in the material's piezoresistivity). The first is the material itself, which was produced originally with the intent to be used for static-controlled packages for sensitive electronics, rather than as a precise sensor substrate. As such, it is made in bulk industrial quantities, and the quality control likely allows for much less uniformity than would be desirable for a sensor, since it would not affect its suitability for the originally intended purpose. The use of a higher quality polymer, intentionally formulated and produced with uniform piezoresistivity in mind, could po-

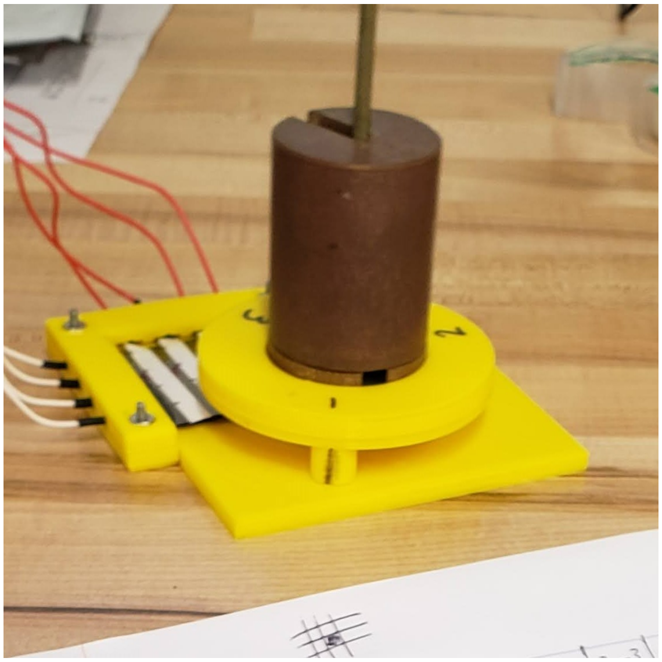

FIG. 5: The test stand used to measure the sensor's response to known pressures.

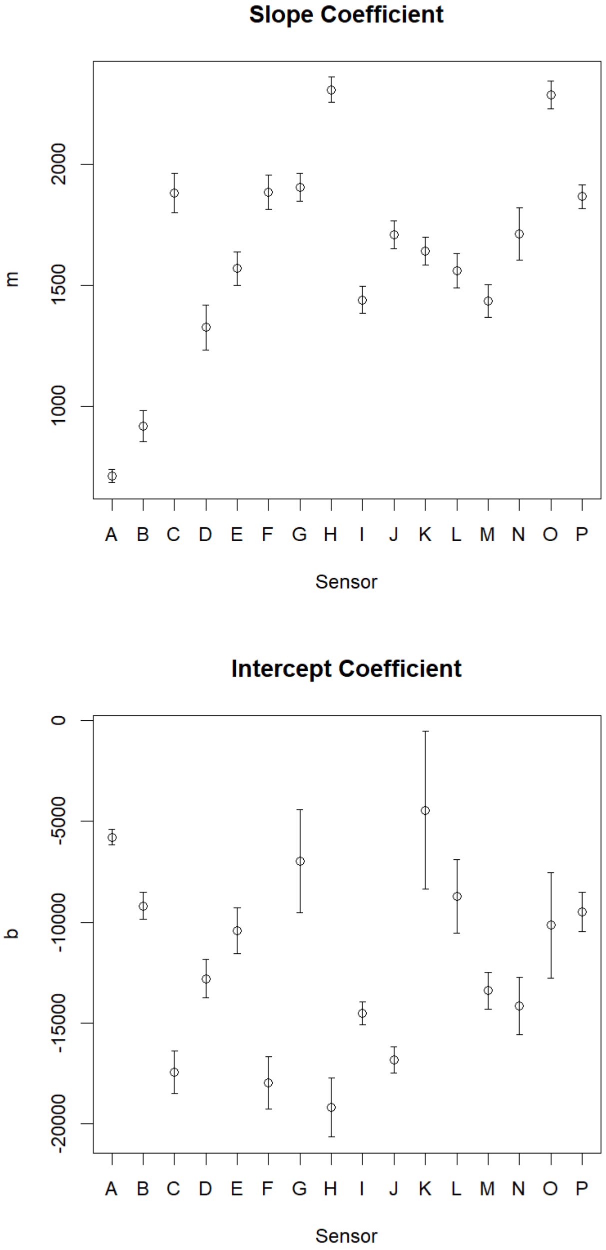

FIG. 6: The coefficients for the linear regression of the form $output^2 = m \cdot pressure + b$.

tentially result in a sensor that has a more uniform response to pressure, rather than varying greatly between pixels as is seen in this study.

The other source of variability in the measurements of this study was the nature of the pressure testing regimen, which consisted of a human placing a known weight on the sensor pixel being tested. Due to unavoidable human error, the pressure was never placed in *exactly* the same spot each trial. The author measuring the data noticed that a difference in positioning of mere millimeters was enough to significantly change the sensor's output (by a factor of 10% or more), so an effort was made the place the mass in the same spot each time, to the best of the tester's ability. If the experiment were to be repeated, the author recommends the use of some sort of jig or template that would ensure the pressure is applied to exactly the same spot in each trial, if not a robotic actuator, in order to guarantee the replicability of the results.

C. Future Experiments

There are several experiments that could be performed in order to more fully understand the properties of this type of sensor and develop better strategies for working around its shortcomings. One possibility that is particularly intriguing would be to try utilizing electrical impedance tomography (EIT)[22], in a similar manner to the system used by Wang et al[18]. This would both reduce the thickness of the sensor in the sensing area (as there would be no need for an electrode lattice on both sides of the polymer sheet) and potentially increase the functional resolution of the sensor itself.

Additionally, one of the benefits of this type of sensor is that it is flexible, so it can be fit onto curved and other irregular surfaces. However, this study was carried out exclusively with the sensor held completely flat. A future experiment that could prove interesting would be to repeat this study with the same sensor measuring pressure on different shaped (non-flat) surfaces, to see if the sensor output is consistent regardless of its configuration.

VII. ACKNOWLEDGMENTS

The project advisor was Dr. Tom Carter, whose guidance, connections, and encouragement were vital to completing the work. Also valuable were the contributions of Dr. Michelle Chen and Dr. Greg Crow, members of the project committee who gave helpful advice on many occasions.

Funding for this project was partially provided by the Point Loma Nazarene University Department of Physics and Engineering as part of their Senior Lab program. The remainder of the project was self-funded by the author.

---

[1] J. M. Waldie, The Mars Society , 1 (2005).
[2] P. Webb and J. F. Annis, *The principle of the space activity suit* (National Aeronautics and Space Administration, 1967).
[3] B. T. Holschuh and D. J. Newman, Aerospace medicine and human performance **87**, 84 (2016).
[4] W. V. Padula, M. K. Mishra, M. B. F. Makic, and P. W. Sullivan, Medical care , 385 (2011).
[5] C.-S. Hu, Y.-F. Chung, C.-C. Yeh, and C.-H. Luo, Evidence-Based Complementary and Alternative Medicine **2012** (2012).
[6] N. Foubert, A. M. McKee, R. A. Goubran, and F. Knoefel, in *2012 IEEE International Symposium on Medical Measurements and Applications Proceedings* (IEEE, 2012) pp. 1–6.
[7] W. Xu, M.-C. Huang, N. Amini, L. He, and M. Sarrafzadeh, IEEE Sensors Journal **13**, 3926 (2013).
[8] H. Z. Tan, L. A. Slivovsky, and A. Pentland, IEEE/ASME Transactions On Mechatronics **6**, 261 (2001).
[9] A. M. Almassri, W. Wan Hasan, S. A. Ahmad, A. J. Ishak, A. Ghazali, D. Talib, and C. Wada, Journal of Sensors **2015** (2015).
[10] H. Morishita, R. Fukui, and T. Sato, in *IEEE/RSJ International Conference on Intelligent Robots and Systems*, Vol. 2 (IEEE, 2002) pp. 1246–1251.
[11] A. G. Kottapalli, M. Asadnia, J. Miao, G. Barbastathis, and M. S. Triantafyllou, Smart Materials and Structures **21**, 115030 (2012).
[12] B. J. Kane, M. R. Cutkosky, and G. T. Kovacs, Journal of microelectromechanical systems **9**, 425 (2000).
[13] "Pressure mapping sensors," `https://www.tekscan.com/pressure-mapping-sensors` (2019), accessed 2020-02-12.
[14] "Pressure measurement film," `https://www.fujifilm.com/products/prescale/`, accessed 2020-02-12.
[15] A. Massaro, F. Spano, A. Lay-Ekuakille, P. Cazzato, R. Cingolani, and A. Athanassiou, IEEE Transactions on Instrumentation and Measurement **60**, 2967 (2011).
[16] M. Nishiyama, H. Sasaki, S. Nose, K. Takami, and K. Watanabe, Materials and Manufacturing Processes **25**, 264 (2010).
[17] M. Esashi, S. Sugiyama, K. Ikeda, Y. Wang, and H. Miyashita, Proceedings of the IEEE **86**, 1627 (1998).
[18] L. Wang, S. Gupta, K. J. Loh, and H. S. Koo, IEEE Sensors Journal **16**, 4663 (2016).
[19] "Velostat," `https://en.wikipedia.org/wiki/Velostat`, accessed 2020-02-12.
[20] "VelostatSensor," `https://github.com/tjwieg/VelostatSensor/`.
[21] R Core Team, *R: A Language and Environment for Statistical Computing*, R Foundation for Statistical Computing, Vienna, Austria (2019).
[22] M. Vauhkonen, W. R. Lionheart, L. M. Heikkinen, P. J. Vauhkonen, and J. P. Kaipio, Physiological measurement **22**, 107 (2001).

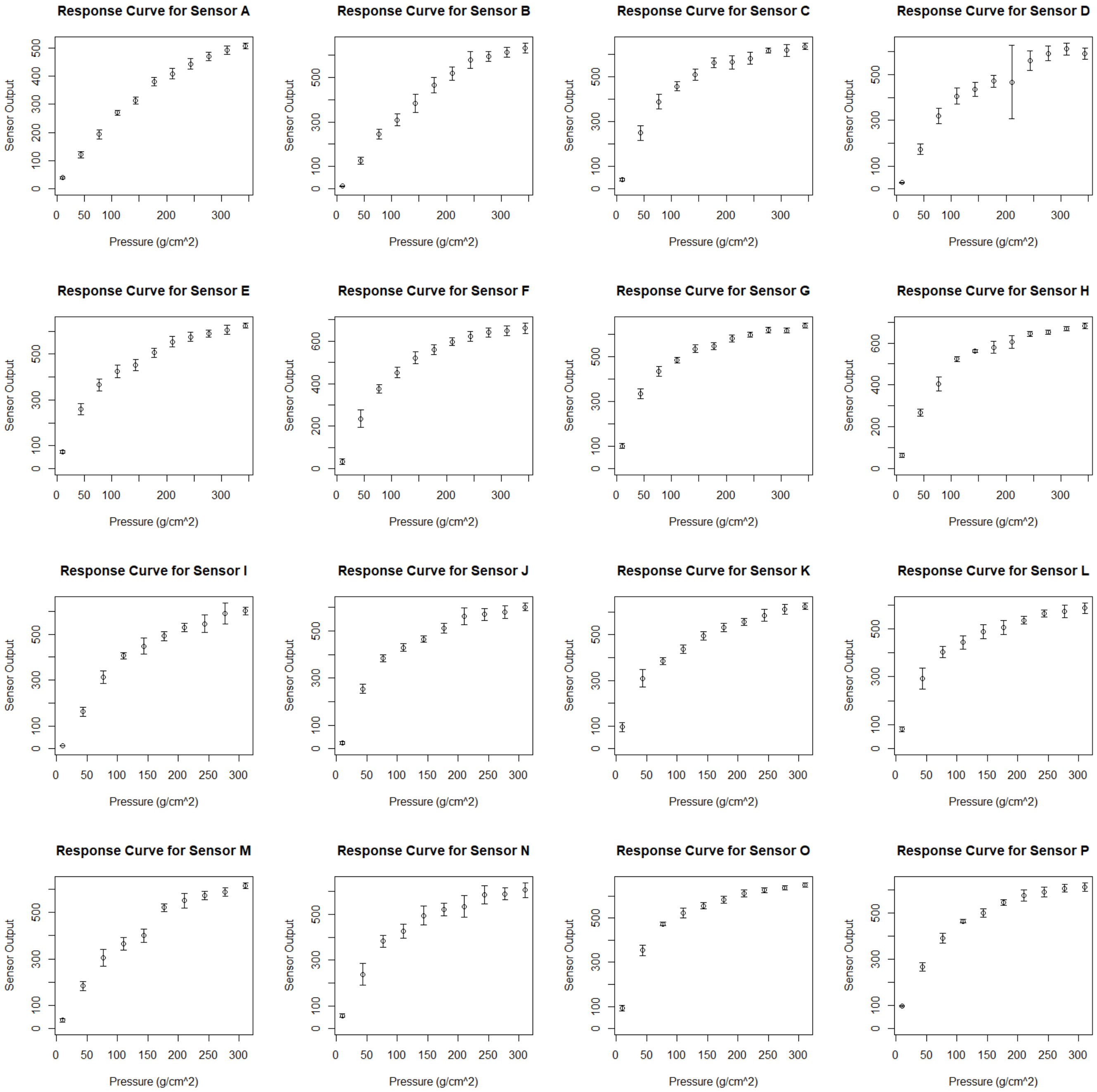

Response Curve for Sensor A
Response Curve for Sensor B
Response Curve for Sensor C
Response Curve for Sensor D
Response Curve for Sensor E
Response Curve for Sensor F
Response Curve for Sensor G
Response Curve for Sensor H
Response Curve for Sensor I
Response Curve for Sensor J
Response Curve for Sensor K
Response Curve for Sensor L
Response Curve for Sensor M
Response Curve for Sensor N
Response Curve for Sensor O
Response Curve for Sensor P

FIG. 7: The average recording from each pixel of the sensor, plotted as a function of pressure. Error bars give the standard deviation.

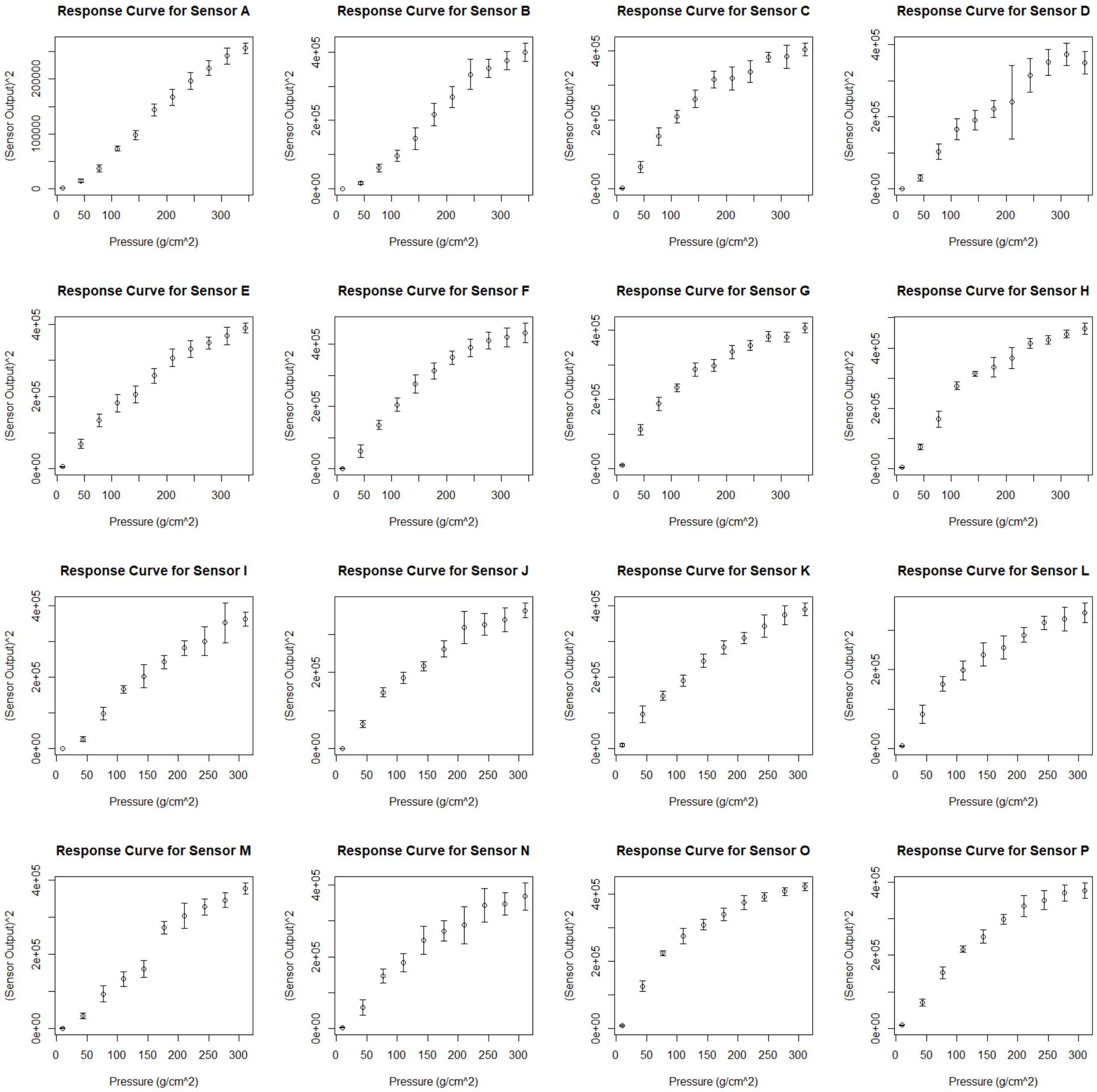

FIG. 8: The average of the square of the recording from each pixel of the sensor, plotted as a function of pressure. Error bars give the standard deviation of the square of the sensor output.

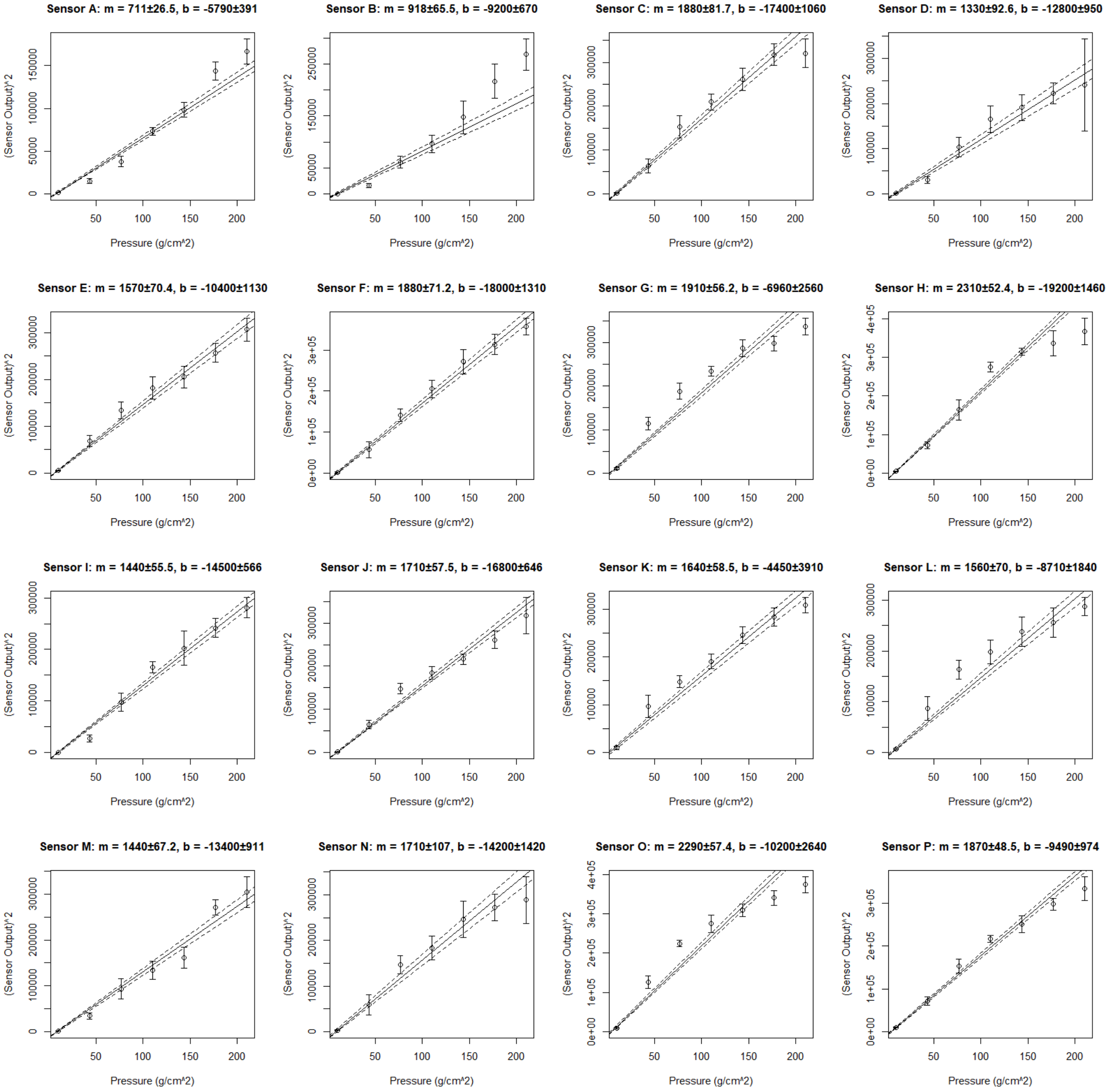
Sensor A: m = 711±26.5, b = -5790±391

Sensor B: m = 918±65.5, b = -9200±670

Sensor C: m = 1880±81.7, b = -17400±1060

Sensor D: m = 1330±92.6, b = -12800±950

Sensor E: m = 1570±70.4, b = -10400±1130

Sensor F: m = 1880±71.2, b = -18000±1310

Sensor G: m = 1910±56.2, b = -6960±2560

Sensor H: m = 2310±52.4, b = -19200±1460

Sensor I: m = 1440±55.5, b = -14500±566

Sensor J: m = 1710±57.5, b = -16800±646

Sensor K: m = 1640±58.5, b = -4450±3910

Sensor L: m = 1560±70, b = -8710±1840

Sensor M: m = 1440±67.2, b = -13400±911

Sensor N: m = 1710±107, b = -14200±1420

Sensor O: m = 2290±57.4, b = -10200±2640

Sensor P: m = 1870±48.5, b = -9490±974

FIG. 9: The first seven data points for the square of the sensor output, plotted as a function of pressure, including a linear regression of the form $output^2 = m \cdot pressure + b$.